



Contents lists available at ScienceDirect

Journal of Microscopy and Ultrastructure

journal homepage: www.elsevier.com/locate/jmau



Original Article

Histological effect of nicotine on adrenal zona fasciculata and the effect of grape seed extract with or without withdrawal of nicotine



Hanaa Attia Khalaf^{a,*}, Fatma M. Ghoneim^a, Eetmad A. Arafat^{a,b}, El-Hassanen M. Mahmoud^c

^a Histology and Cell Biology Department, Faculty of Medicine, Mansoura University, Egypt

^b Department of Anatomy, Taif University, Saudi Arabia

^c Psychiatry Department, Faculty of Medicine, Mansoura University, Egypt

ARTICLE INFO

Article history:

Received 29 August 2016

Accepted 5 November 2016

Available online 15 December 2016

Keywords:

grape seed extract

nicotine

nicotine withdrawal

zona fasciculata

ABSTRACT

Cigarette smoking is harmful to the health of both smokers and nonsmokers. It is a major cause of death. This study aimed to investigate the structural changes in the zona fasciculata of albino rats caused by nicotine and the protective effect of grape seeds with or without the stoppage of nicotine administration. Thirty-five adult male rats were used and equally divided into five groups: negative and positive control groups (Groups I and II), nicotine-treated group (Group III), nicotine- and grape seed extract-treated group (Group IV), and nicotine withdrawal and grape seed extract-treated group (Group V). Adrenal glands were dissected and prepared for histological studies. The majority of zona fasciculata cells of Group III showed striking changes in terms of swelling of the cells with marked cytoplasmic vacuolation, many pyknotic nuclei, and increased immunoexpression to caspase 3 antibodies. By electron microscopy, a marked increase in lipid deposition with its appearance in the capillary between zona fasciculata cells was noticed. Heterochromatic nuclei and dilated smooth endoplasmic reticulum were noted. Degenerated mitochondria and some mitochondria that had cavitation with a progressive loss of their cristae were seen. The zona fasciculata cells of Group IV were partially improved, while in Group V, those cells showed complete improvement. We can conclude that nicotine causes severe histological changes in zona fasciculata cells. Grape seed extract can partially ameliorate these changes, and complete recovery is achieved with grape seed extract after the stoppage of nicotine administration.

© 2016 Saudi Society of Microscopes. Published by Elsevier Ltd. This is an open access article under the CC BY-NC-ND license (<http://creativecommons.org/licenses/by-nc-nd/4.0/>).

Introduction

Many thousands of components are present in a cigarette. Nicotine is one of the few liquid alkaloids that are

commonly absorbed by the body through cigarette smoking (a cigarette contains approximately 2 mg of absorbed nicotine) [1,2] and tobacco ingestion (nicotine represents roughly 0.6–3.0% of the dry weight of tobacco) [3]. Nicotine exists as a powerful parasympathomimetic alkaloid in the nightshade group of plants and is also found in the leaves of *Nicotiana rustica* [4]. Various studies indicated that nicotine causes a critical rise in serum cortisol, then cortisol levels fall with time as well as during the early

* Corresponding author. Histology and Cell Biology Department, Faculty of Medicine, Mansoura University, El Gomhoria Street, Mansoura City, Egypt.

E-mail address: ok67203964949@yahoo.com (H.A. Khalaf).

withdrawal process [5]. In the adrenal medulla, nicotine binds to its receptors, leading to increased heart rate, blood pressure, respiratory rate, and blood glucose levels caused by increased adrenaline and noradrenaline secretion [6]. In lesser doses, nicotine acts as a stimulant, while it can be risky at a high dose (> 50 mg). This stimulating effect makes nicotine highly addictive. This addictiveness of nicotine is the main reason for the persistent usage of tobacco products, which in turn results in most of the tobacco-related diseases [7].

Nicotine is associated with cardiovascular disease, congenital anomalies, and poisoning [8]. Moreover, nicotine has been found to distract the antioxidant defense mechanisms in rats [9,10]. Oxidation is a chemical reaction that can create free radicals (such as superoxide, nitric oxide, and hydroxyl ions) all of which have an unpaired electron. During normal metabolism, free radicals are created, and their levels are enhanced during contact with environmental pollutants such as cigarette smoke [11]. Fats in the cell membrane are susceptible to damage by these free radicals. These electrons can start new reactions, and it is known as reactive oxygen species. In turn, oxidation causes death of or damage to the cell. Antioxidants suppress these effects through the removal of free radicals and inhibition of other oxidative reactions [12]. The reactive oxygen species are offset naturally by antioxidant defense factors, such as superoxide dismutase, which already exist in our body under physiological conditions. During oxidative stress, oxidant factors outstrip natural antioxidant factors. Consequently, it causes destructive processes that can lead to cell death [13].

Grape (*Vitis vinifera*) is one of the extensively consumed fruits in the world. Grape has many active gradients, including flavonoids, polyphenols, anthocyanins, proanthocyanidins, and procyanidins [14]. It was hypothesized that proanthocyanidin extract acts as a free radical scavenger and an antioxidant [15]. Further, grape modifies a lot of biological reactions, and it has anti-inflammatory, anticarcinogenic, and antiaging effects; therefore, it is considered a cytoprotective agent [16].

The hazardous effect of nicotine regarding the morphological changes in the adrenal cortex is still not well established. Accordingly, the aim of the present study is to investigate the structural changes caused by nicotine administration to the adrenal zona fasciculata (ZF) cells of albino rats, as well as the possible protective effect of grape seeds, with or without the stoppage of nicotine administration, on these changes.

Materials and methods

Chemicals

Nicotine was purchased from Sigma Chemical Co. (St. Louis, MO, USA) in the form of powder {nicotine hydrogen tartrate salt [(-)-1-methyl-2-(3-pyridyl) pyrrolidine (+)-bitartrate salt]}. Nicotine was dissolved in distilled water.

Grape seed extract (GSE) was purchased from Arab Gelatin Pharmaceutical Products Company, Alexandria, Egypt. It was dissolved in saline.

Investigational protocol

The protocol of this study was accepted by the Ethical Committee of the Faculty of Medicine, Mansoura University, Mansoura City, Egypt.

The present study included 35 adult male rats (each weighing about 180–200 g) (Nile Research Center – El Teraa Street, Mansoura City). Prior to the study, the animals were kept in a quiet and nonstressful environment for 1 week. Animals were fed *ad libitum* and permitted free access to water throughout the investigational time. Rats were divided equally into five groups (7 rats in each group): Group I (negative control group): Animals were given saline via intragastric tube and injected subcutaneously with distilled water for 1 month. Group II (positive control group): Animals received GSE daily (at a dose 200 mg/kg body weight/d), dissolved in saline, via an intragastric tube for 1 month [17]. Group III (nicotine-treated group): Animals were given nicotine powder liquefied with distilled water and injected subcutaneously at 2.5 mg/kg/d [18] for 1 month. Group IV (nicotine- and GSE-treated group): Animals were simultaneously given GSE (at the same dose as that of Group II) and nicotine (at a dose similar to that of Group III) for 1 month. Group V (nicotine withdrawal and GSE-treated group): Each animal received the same dose of nicotine and GSE as those of Group IV for 1 month; they were studied 2 months after the stoppage of nicotine administration to assess its withdrawal effect.

After each experiment, animals were sacrificed. Partial fixation of specimens was done by intracardiac perfusion using 2.5% phosphate buffered glutaraldehyde (PH 7.4). Adrenal glands were dissected, weighted, and prepared for histological, immunohistochemical, and electron microscopic studies.

Histological study

The right adrenal glands were cut and fixed in Bouin's solution. Then, dehydration of the specimens in alcohol was done, followed by clearing in xylene and embedding in paraffin. Using a rotary microtome, sections of 5 μm thickness were obtained, which were placed on clean slides. Next, slides were stained with hematoxylin and eosin according to the method of Bancroft and Layton [19].

Immunohistochemical study

Sections were placed on positive slides and then immunostained by the avidin–biotin technique [20]. Deparaffinization and rehydration of the slides were performed, followed by rinsing in tap water. For blocking of endogenous peroxidase activity, the slides were embedded in 0.01% H_2O_2 ; then the antigenic site was unmasked by putting sections in 0.01 M citrate buffer (pH 6) for 30 minutes. After that boiling was done in a microwave for 6 minutes. To omit nonspecific background, the slides were incubated for 20 minutes in diluted normal rabbit serum, followed by incubation in primary antibody (caspase 3/CPP32 rabbit polyclonal antibody) at 1/50–1/100 dilution for 2 hours. Subsequently, the slides were incubated using the avidin–biotin complex substrate for 60 minutes and

Table 1

Adrenal weight of the studied group.

Group I	Group II	Group III	Group IV	Group V	p
0.30 ± 0.006	0.030 ± 0.008	0.060 ± 0.010	0.035 ± 0.006	0.032 ± 0.007	0.918* < 0.001** 0.222*** 0.560****

* Group I versus Group II.

** Group I versus Group III; significant.

*** Group I versus Group IV.

**** Group I versus Group V

then in peroxidase substrate solution for 6–10 minutes. Lastly, counterstaining by hematoxylin was performed. For the negative control slide, the used 1ry antibody was exchanged by phosphate buffer saline. Tonsil was considered positive control [21].

The polyclonal rabbit caspase 3/CPP32 antibody [Diagnostic Biosystems, Pleasanton, CA, USA (format: purified immunoglobulin fraction of rabbit antiserum against caspase 3; Emergo Europe, the Hague, The Netherlands)] was used for staining the cytoplasmic antigens.

Electron microscopic study

Small pieces of the left adrenal cortex were used for transmission electron microscopy and fixed for 2 hours in 2.5% glutaraldehyde buffered with 0.1 M cacodylate at pH 7.2; then the specimens were washed by this buffer. Then postfixation at the room temperature was performed by 1% osmium tetroxide buffered with phosphate for 2 hours, followed by alcohol dehydration. Specimens were embedded in epoxy resin mixture, after immersion in propylene oxide. Semi-thin sections of about 1 μm thickness were cut, stained by 1% toluidine blue, and then examined with a light microscope. Next, ultrathin sections (80–90 nm) were obtained using an LKB ultratome, and stained by uranyl acetate and lead citrate [22]. The ultrastructural analysis was done using a transmission electron microscope (Joel TEM CS 100 - JOES (Germany) GmbH Gute Anger 30 DE-85356, Freising, Germany) in the Electron Microscopic Unit, Faculty of Science, El-Shatby, Alexandria University, Egypt.

Morphometric study

By image analyses, the area percent of the immunoreaction of the studied group was evaluated using five immune-stained slides for every group. The slides were photographed with an Olympus digital camera (E24-10

mega pixel; Olympus, China) fitted on an Olympus microscope through a 0.5× photo adaptor, using a 40× objective lens. The resulted images were evaluated by an Intel Core 13 computer using Video Test Morphology software (Video Test, Saint Petersburg, Russia) using a specific built-in routine for calculating the area percent of immunoreaction [23].

Biochemical study

Blood was collected from the left ventricle of the rats to measure the level of malondialdehyde (MDA) [24].

Statistical analysis

Weights of adrenal, morphometric, and biochemical data were evaluated using the Student *t* test, and calculated as mean value ± standard deviation. A probability value of *p* < 0.05 was considered significant and *p* < 0.01 highly significant [25].

Result

Statistical data

In Table 1, the adrenal weight of group III was significantly increased compared with that of the control groups. In addition, the adrenal weight of Group IV was increased compared with that of the control groups, but this increase was statistically nonsignificant. However, the adrenal weight of Group V was similar to that of the control groups.

The serum level of MDA was significantly increased in Group III compared with that in Group I. Moreover, a non-significant increase of the serum level of MDA was detected in Group IV compared with that of Group I, but the MDA level of Group V was similar to that of Group I (Table 2).

Table 2

Level of serum MDA of the studied group.

Group I	Group II	Group III	Group IV	Group V	p
4.71 ± 0.64	4.81 ± 0.62	11.89 ± 3.03	5.55 ± 0.94	4.73 ± 0.61	0.902* < 0.001** 0.073*** 0.978****

* Group I versus Group II.

** Group I versus Group III.

*** Group I versus Group IV; significant.

**** Group I versus Group V.

MDA = malondialdehyde.

The area percent of immunoexpression of caspase 3 was significantly increased in Group III and nonsignificantly increased in Group IV compared with the control groups. This value in Group V was similar to that in Group I (Table 3).

Histological result

Light microscopic examination

Examination of the hematoxylin and eosin-stained sections of the control groups revealed the normal histological architecture of the ZF. The ZF was the middle and the broadest zone of the adrenal cortex. It was placed between the zona glomerulosa and the zona reticularis (Figure 1A). Cells of the ZF were arranged in parallel cords separated by blood

sinusoids, and the cords were of one or two cells in width. The cells were polyhedral with central, rounded vesicular nuclei. The cytoplasm was faintly stained acidophilic and vacuolated. Binucleated cells could be seen (Figure 1B). Immunostained sections showed weak positive and minimal cytoplasmic reactions to caspase 3 of the ZF cells (Figure 2A).

In the nicotine-treated group (Group III), there was a disorganization of the ZF arrangement. The majority of the ZF cells showed striking changes in the form of swelling of the cells with marked cytoplasmic vacuolation. Many nuclei appeared pyknotic, and dilatation of blood sinusoids were observed (Figures 1C and 1D). In the immunostained sections, increased immunoexpression of the ZF

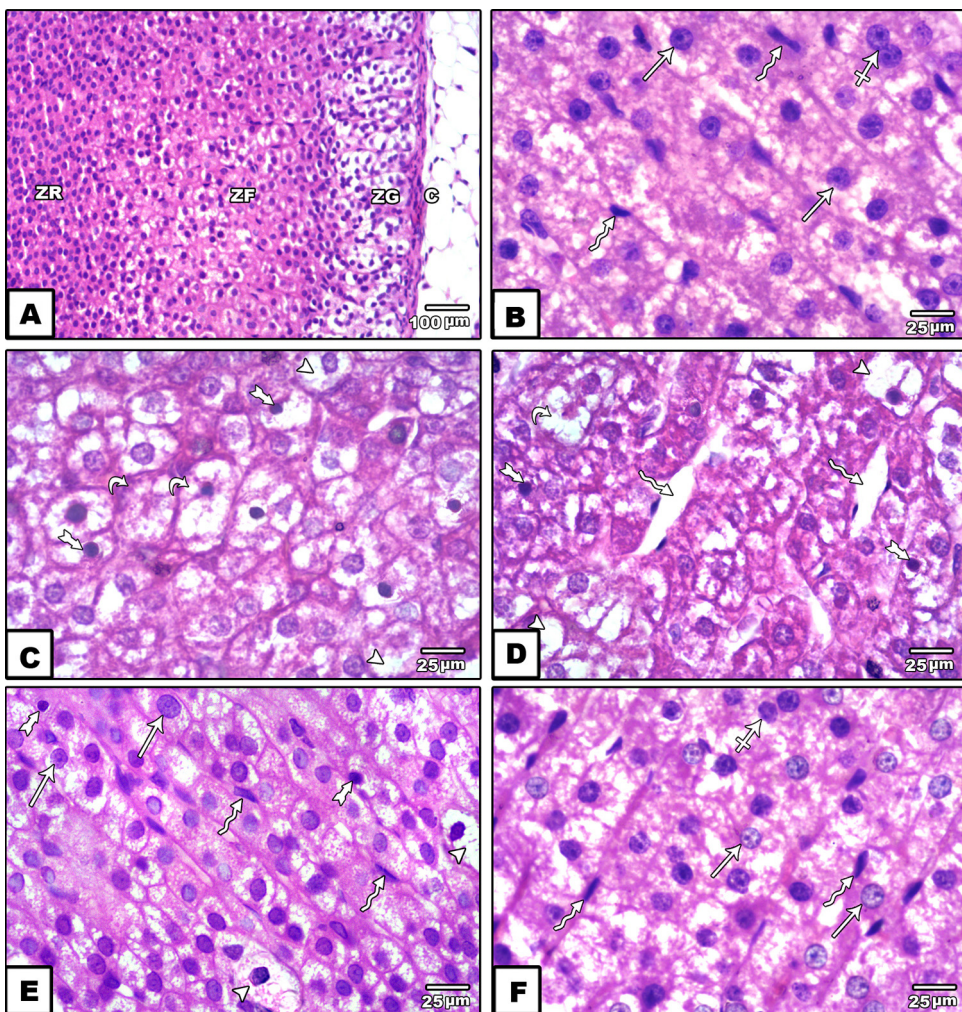


Fig. 1. (A,B) Sections stained with H&E (Group 1; Control group). The suprarenal cortex of Group I showing thick capsule, ZG, ZF, and ZR. ZF shows polyhedral cells arranged in parallel cords disjoined by blood sinusoids (zigzag arrows). The cords are one or two cells in width. The cells have central, rounded vesicular nuclei (arrows) and vacuolated, faintly stained acidophilic cytoplasm. Binucleated cells (crossed arrow) are seen. (C,D) Some swollen cells (curved arrows) with cytoplasmic vacuolation (arrow heads) are noticed in the ZF of Group III (nicotine-treated group). Many pyknotic nuclei (tailed arrows) are seen. Note the appearance of dilated blood sinusoids (zigzag arrows). (E) Most of the ZF cells of Group IV (nicotine- and GSE-treated group) are normal. The cells are polyhedral and arranged in parallel cords disjoined by blood sinusoids (zigzag arrow). The cells have central rounded vesicular nuclei (arrows) and vacuolated, faintly stained acidophilic cytoplasm. Note the appearance of a few pyknotic nuclei (tailed arrows) and cytoplasmic vacuolation (arrow heads). (F) ZF cells of group V (nicotine withdrawal and GSE-treated group) showing a normal histological structure of the ZF. The cells are polyhedral and arranged in parallel cords disjoined by blood sinusoids (zigzag arrow). The cells have central, rounded vesicular nuclei (arrows) and faintly stained acidophilic vacuolated cytoplasm. Binucleated cells (crossed arrow) can be seen.

C = capsule; GSE = grape seed extract; H&E = hematoxylin and eosin; ZF = zona fasciculata; ZG = zona glomerulosa; ZR = zona reticularis.

Table 3

Area percentages of the caspase 3 immunoexpression of the studied group.

Group I	Group II	Group III	Group IV	Group V	<i>p</i>
3.09 ± 0.61	2.87 ± 0.55	41.97 ± 10.91	6.29 ± 0.88	4.66 ± 0.60	0.934* < 0.001** 0.233*** 0.555****

* Group I versus Group II.

** Group I versus Group III; significant.

*** Group I versus Group IV.

**** Group I versus Group V.

cells to caspase 3 antibodies was prominently observed (Figure 2B).

In comparison with Group III, the light microscopic examination of hematoxylin and eosin-stained sections of the nicotine- and GSE-treated group (Group IV) revealed a normal architecture of the cortex. However, a few ZF cells were swollen, and others had pyknotic nuclei and vacuolated cytoplasm (Figure 1E). The immunostained sections of the ZF cells of this group showed a mild positive cytoplasmic reaction to caspase 3 antibodies (Figure 1C).

In the nicotine withdrawal and GSE-treated group (Group V), the ZF showed an almost normal histological structure. The cells were arranged in parallel cords separated by blood sinusoids. The cells were polyhedral with central, rounded vesicular nuclei and faintly acidophilic vacuolated cytoplasm (Figure 1F). Examination of the immunostained sections of this group revealed a reaction almost similar to that of the control groups where there

was a minimal positive cytoplasmic reaction to caspase 3 antibodies in the ZF (Figure 2D).

Electron microscopic results

Examination of the ultrathin sections of the control groups showed the normal ultrastructural image of the ZF cells. The nucleus was euchromatic with prominent nucleolus. The mitochondria were spherical and variable in size with densely packed vesicular cristae. Plenty of smooth endoplasmic reticulum (sER) tubules and a lipid droplet were seen (Figure 3A).

The ZF of Group III showed a marked increase in lipid deposition, with the appearance of a lipid droplet in the capillary between the ZF cells (Figure 3B). Some nuclei had irregular outlines with condensed chromatin (Figures 3B and 3E) and others were heterochromatic (Figures 3C and 3D). Many degenerated mitochondria (Figure 3D), bizarre-shaped mitochondria (Figure 3D), and some mitochondria

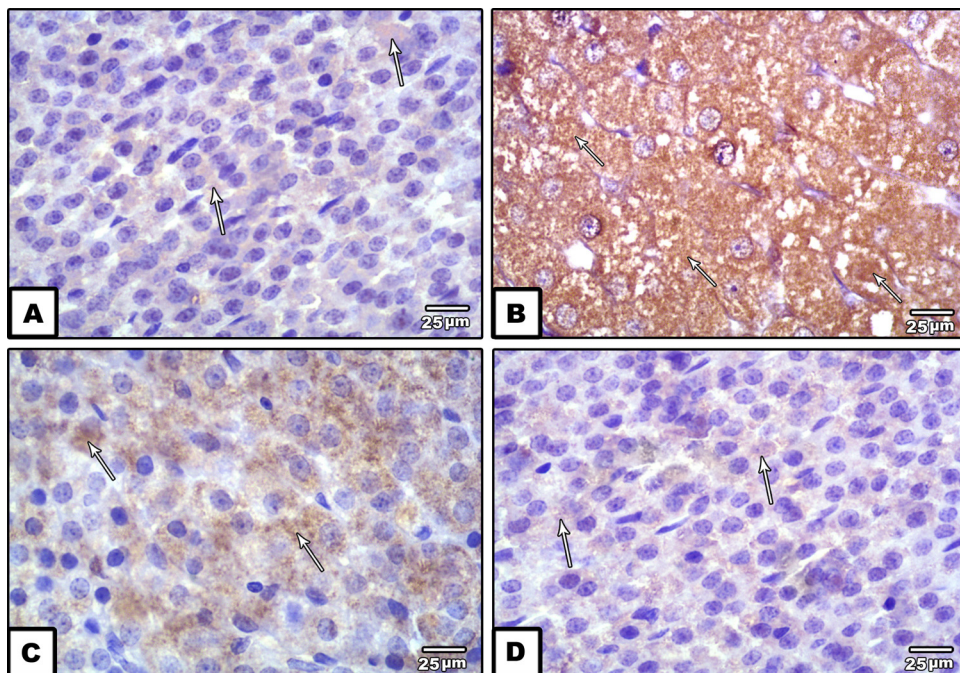
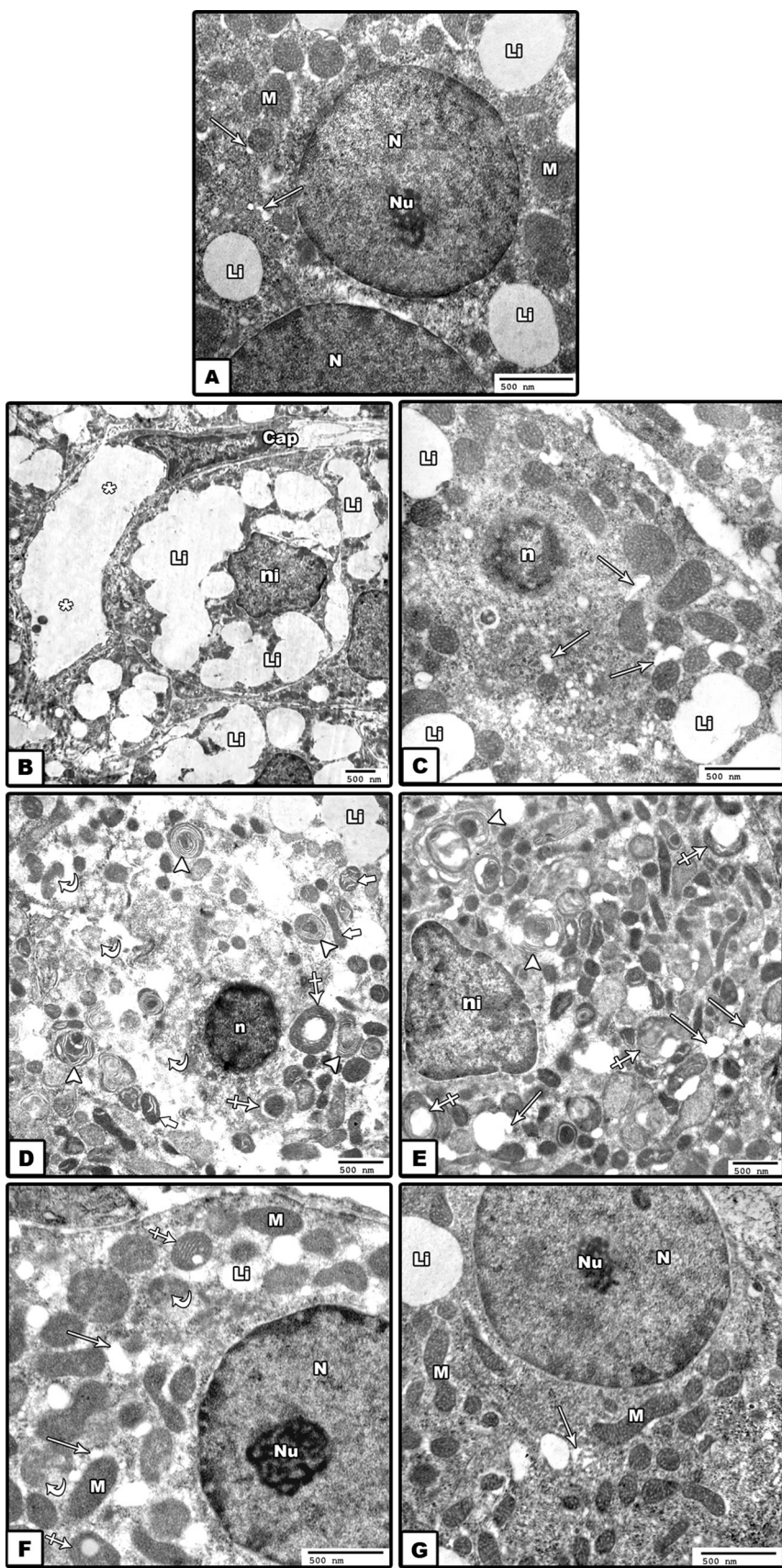


Fig. 2. Immunostained sections. (A) The ZF of Group I (Control group) showing a minimal positive cytoplasmic reaction to caspase 3 antibodies (arrows). (B) The ZF of Group III (nicotine-treated group) showing a marked increase in the cytoplasmic reaction to caspase 3 antibodies (arrows). (C) The ZF of group IV (nicotine- and GSE-treated group) showing a mild positive cytoplasmic reaction to caspase 3 antibodies in ZF cells (arrows). (D) The ZF of Group V (nicotine withdrawal and GSE-treated group) showing a minimal positive cytoplasmic reaction to caspase 3 (arrows). GSE = grape seed extract; ZF = zona fasciculata.



possessing cavitation with a progressive loss of their cristae (Figures 3D and 3E) were all seen with dilated sER (Figures 3C and 3E). Many autophagic bodies (Figures 3D and 3E) were detected.

Ultrastructural examination of the ZF cells of Group IV showed a nearly normal structure of the ZF cells. Euchromatic nucleus with a prominent nucleolus and a few lipid droplets were seen. However, few mitochondria were degenerated and others were vacuolated. Moreover, some dilated sER were detected (Figure 3F).

An electron microscopic image of the ZF cells of Group V showed an almost normal histological structure. An euchromatic nucleus, a few lipid droplets, and sER were seen. Mitochondria were spherical and variable in size with densely packed vesicular cristae (Figure 3G).

Discussion

Cigarette smoking is harmful to the health of both smokers and nonsmokers. It is a major cause of death, accounting for one in five deaths in the United States [26]. Nicotine is one of the dangerous components of a cigarette [27]. Its biological effects are widespread and extend to all systems of the body including cardiovascular, respiratory, renal, and reproductive systems. In several studies, nicotine has also been found to be carcinogenic [6]. Furthermore, nicotine has been found to distract the antioxidant defense mechanisms in rats, and increase lipid peroxidation and deplete antioxidants in tissues [9,10].

The current study was carried out to investigate the structural changes caused by nicotine administration to the adrenal ZF cells, as well as the possible effect of grape seeds with or without the stoppage of nicotine administration.

In our work, the majority of the ZF cells of the rats treated by nicotine (Group III) showed destructive structural and ultrastructural changes. The most striking changes detected were in the form of swelling of cells, marked cytoplasmic vacuolation, and a marked increase in lipid deposition. Some mitochondria were degenerated and others possessed cavitation with a progressive loss of cristae. Many pyknotic shrunken nuclei were seen, and it was proved by a significant increase in the area percent of the caspase 3-stained sections. Dilated sER and many autophagic vacuoles containing degenerated mitochondria could be detected.

This result was in harmony with those of other authors; Osman [18] reported that accumulation of lipid droplets and appearance of cytoplasmic vacuolation in the ZF cells after treatment with nicotine may be due to the impairment in the synthesis of glucocorticoids. As the ZF is

responsible for synthesis and secretion of glucocorticoids, the disrupted steroidogenesis had a vital role in the toxicity of the adrenal cortex. This may occur as a result of disruption of cytochrome P450 enzymes; therefore, cholesterol biosynthesis will be inhibited. This will lead to accumulation of lipid droplets and cytoplasmic vacuolation of the ZF cells [28]. This also was constant with the data of previous researchers who noticed accumulation of lipid droplets in the cells of the ZF and zona reticularis after suppression of steroidogenesis via dexamethasone administration [29].

The adrenal gland expresses the level-limiting enzyme of steroidogenesis, acute regulatory protein (StAR), and cytochrome P450 cholesterol side chain cleavage (P450scc), which is crucial for the secretion of steroid hormones [30]. StAR settles the passage of cholesterol from the outer to the inner mitochondrial membrane, which is the first and rate-limiting stage in steroid synthesis, while P450scc splits the cholesterol side chain, converting cholesterol to pregnenolone, the predecessor of steroid hormones [31]. It was found that nicotine treatment repressed StAR/P450scc expressions, thereby inhibiting cortisol secretion. Furthermore, the expression of StAR stayed inhibited more than 15 days after the stoppage of nicotine treatment [32].

Another investigator stated that the swelling and vacuolation that was detected in the mitochondria of the ZF cells possibly resulted from the suppression of cholesterol to pregnenolone conversion. Consequently, cholesterol accumulates within the mitochondria. Subsequently, it undergoes significant hypertrophy and cavitation [28].

As the mitochondria and sER play important roles in steroidogenesis, the lesions detected in them were sufficient to inhibit steroid synthesis, leading to further accumulation of cholesterol in the mitochondria.

The two main apoptotic ways within a cell are the extrinsic pathway (receptor pathway) and the intrinsic one (mitochondrial pathway). The intrinsic pathway is triggered by many intrinsic signals including oxidative stress via the involvement of the mitochondria [33]. Caspase 3 is activated by both extrinsic and intrinsic pathways, so it is used as an apoptotic marker.

Many studies revealed that caspase 3 immunoreaction was increased by apoptosis [34]. Moreover, nicotine activated specific intracellular death-related pathways, leading to increased caspase 3 immunoreaction in Leydig cells [35]. These findings are also in close agreement with that presented by Machaalani and colleagues [36], who observed that postnatal nicotine exposure can lead to increased caspase 3 reaction in the hypoglossal, gracile, and dentate gyrus of the brain of male piglets. Increased caspase

Fig. 3. Electron micrographs. (A) The ZF of Group I (Control group) showing a binucleated cell. The nuclei are euchromatic (N) with a prominent nucleolus (Nu). The mitochondria (M) are spherical, variable in size with densely packed vesicular cristae. The sER tubules (arrows) and a lipid droplet (Li) are seen. (B–E) The ZF of Group III (nicotine-treated group) showing a marked increase in the lipid deposition (Li) with the appearance of lipid droplets (asterisks) in the capillary (Cap) between the ZF cells. Some nuclei have irregular outlines with condensed chromatin (ni) and others are heterochromatric (n). Many degenerated mitochondria (curved arrows), bizarre-shaped mitochondria (thick arrows), and some mitochondria possessing cavitation with a progressive loss of their cristae (crossed arrow) all are seen with dilated sER (arrows). Many autophagic bodies (arrow heads) are detected. (F) ZF cells of group IV (nicotine- and GSE-treated group) showing euchromatic nucleus (N) with a prominent nucleolus (Nu) and a few lipid droplets (Li). Many mitochondria (M) are normal, while few are degenerated (curved arrows) and others are vacuolated with the loss of their cristae (crossed arrow). Note the presence of dilated sER (arrows). (G) ZF cells of group V (nicotine withdrawal and GSE-treated group) showing euchromatic nucleus (N) with a prominent nucleolus (Nu) and a few lipid droplets (Li). Mitochondria (M) are variable in size with densely packed cristae. Note the presence of sER (arrows). GSE = grape seed extract; sER = smooth endoplasmic reticulum; ZF = zona fasciculata.

3 expression was detected in human gingival fibroblasts treated with nicotine due to decreased cell integrity and increased apoptosis [37].

In the present study, there was a statistically significant increase in the adrenal weight and the serum level of MDA of Group III compared with that of Group I.

Enlargement of the adrenals suggests the possibility of cellular damage by nicotine, leading to accumulation of lipids in adrenal cells and swelling of cell organelles (as seen on the histological sections) and hence an increase in the adrenal weight.

These data were confirmed previously by Iranloye and Bolarinwa [38]. They noticed that there was an increase in the weights of adrenals after 30 days of nicotine administration.

MDA is a predictor of lipid peroxidation (used as a marker for the detection of tissue damage caused by free radicals); so the increased serum level of MDA observed in the present work suggests that nicotine induces oxidative stress. The current results were in agreement with the data of Razali and colleagues [39] who announced that fat and cholesterol of the cell membrane are targets of free radical attack; hence, lipid peroxidation can occur, as evident from the increased MDA level. These data also coincide with that attained by Parlakpinar and colleagues [40] who stated that, in normal circumstances, reactive oxygen species are eradicated by intrinsic antioxidant enzymes such as superoxide dismutase, catalase, and glutathione peroxidase. This is achieved by increased MDA levels and a decrease in superoxide dismutase activity.

Nicotine is considered a potent oxidant as it produces free radicals that react with the cell membrane, leading to oxidative damage and cellular death [41].

Moreover, it was established that nicotine induces oxidative stress both *in vitro* and *in vivo*, increasing the amounts of free radicals and lipid peroxidation products in cultured cells [42]. Nicotine is first oxidized into cotinine in the liver, generating free radicals and inducing oxidative injury to tissues [43].

The findings of the present work revealed a normal architecture of the ZF of Group IV, in spite of the presence of a few swollen cells with pyknotic nuclei and vacuolated cytoplasm. Degenerated and vacuolated mitochondria were also detected. There was a mild positive cytoplasmic reaction to caspase 3 antibody that was proved by the morphometric analysis. In addition, the adrenal weight and serum level of MDA of Group IV were nonsignificantly increased compared with those of Group I.

From these results, it was evident that the ameliorative effect of GSE is possibly due to its antioxidant potency.

These results agree with those published by Ahmed and colleagues [44] who revealed that GSE protects the rat liver against hepatotoxins and reduces liver MDA. They postulated that this was due to the action of GSE as a free radical scavenger. Also, Zhang et al [45] stated that GSE is a potent antioxidant, and prevents arsenic-induced renal fibrosis and dysfunction. Furthermore, it was found that GSE protects many organs (heart, kidney, and liver) from the oxidative stress of cisplatin [17].

GSE is a source of proanthocyanidins, a class of phenolic compounds that increase intracellular vitamin C levels,

decrease capillary permeability, act as free radicals scavengers, and inhibit lipid peroxidation [46].

The structure of the ZF cells of Group V of our work was integral to the architecture of Group I. Furthermore, there was a minimal positive immunoreaction to caspase 3 antibody similar to that of the control groups and it was confirmed by the morphometric analysis. Moreover, the adrenal weight and serum level of MDA of this group were similar to those of Group I.

Similar results were obtained by Nesseim et al [47], who stated that the histological changes of seminiferous tubules of rats were partially recovered after nicotine withdrawal, particularly at small doses (0.2 mg nicotine per day). In addition, these data were in agreement with the data of El-Meligy et al [48], who announced that stoppage of nicotine administration leads to partial improvement of ovarian and uterine destructive changes. They added that complete recovery may occur if the stoppage was accompanied by an antioxidant therapy.

Conclusion

From the previous results, we can conclude that nicotine causes severe histological and biochemical changes of the ZF cells. These changes are based mainly on the oxidative stress potentiality of nicotine; GSE can partially ameliorate these changes. However, complete recovery is obtained with GSE after the stoppage of nicotine administration.

We recommend that it is necessary to stop smoking due to its hazardous effects, and an antioxidant must be given after the stoppage of nicotine use to gain complete recovery.

Conflicts of interest

None.

References

- [1] Girma E, Assefa T, Deribew A. Cigarette smoker's intention to quit smoking in Dire Dawa town Ethiopia: an assessment using the trans-theoretical model. BMC Public Health 2010;10:320.
- [2] Mayer B. How much nicotine kills a human? Tracing back the generally accepted lethal dose to dubious self-experiments in the nineteenth century. Arch Toxicol 2014;88:5–7.
- [3] Rodgman A, Perfetti TA. The chemical components of tobacco and tobacco smoke. Boca Raton, FL: CRC Press; 2009.
- [4] Malenka RC, Nestler EJ, Hyman SE. Autonomic nervous system. In: Sydor A, Brown RY, editors. Molecular neuropharmacology: a foundation for clinical neuroscience, 9, 2nd ed. New York: McGraw-Hill Medical; 2009. p. p234.
- [5] Kapoor D, Jones TH. Smoking and hormones in health and endocrine disorders. Eur J Endocrinol 2005;152:491–9.
- [6] Mishra A, Chaturvedi P, Datta S, Sinukumar S, Joshi P, Garg A. Harmful effects of nicotine. Indian J Med Paediatr Oncol 2015;36:24–31.
- [7] Shihadeh A, Saleh R. Polycyclic aromatic hydrocarbons, carbon monoxide, "tar", and nicotine in the mainstream smoke aerosol of the narghile water pipe. Food Chem Toxicol 2005;43:655–61.
- [8] Jerry JM, Collins GB, Strem D. E-cigarettes: safe to recommend to patients? Cleve Clin J Med 2015;82:521–6.
- [9] Kalpana C, Rajasekharan KN, Menon VP. Modulatory effects of curcumin and curcumin analog on circulatory lipid profiles during nicotine-induced toxicity in Wistar rats. J Med Food 2005;8:246–50.
- [10] Perlemer G, Davit-Spraul A, Cosson C, Conti M, Bigorgne A, Paradis V, et al. Increase in liver antioxidant enzyme activities in non-alcoholic fatty liver disease. Liver Int 2005;25:946–53.

- [11] Zeidler R, Albermann K, Lang S. Nicotine and apoptosis. *Apoptosis* 2007;12:1927–43.
- [12] Wang Z, Li S, Cao Y, Tian X, Zeng R, Liao DF, et al. Oxidative stress and carbonyl lesions in ulcerative colitis and associated colorectal cancer. *Oxid Med Cell Longev* 2016;2016:9875298.
- [13] Ibukun EO, Oladipo GO. Lipidomic modulation in stressed albino rats is altered by yolk and albumen of quail (*Coturnix japonica*) egg and poultry feed. *Biochem Res Int* 2016;2016. Article ID 2565178, 7 pages.
- [14] Lazzè MC, Pizzala R, Gutiérrez Pecharromán FJ, Gatón Garnica P, Antolín Rodríguez JM, Fabris N, et al. Grape waste extract obtained by supercritical fluid extraction contains bioactive antioxidant molecules and induces antiproliferative effects in human colon. *J Med Food* 2009;12:561–8.
- [15] Uchida S, Hirai K, Hatanaka J, Hanato J, Umegaki K, Yamada S. Antinociceptive effects of St. John's wort, *Harpagophytum procumbens* extract and grape seed proanthocyanidins extract in mice. *Biol Pharm Bull* 2008;31:240–5.
- [16] Wang H, Xue Y, Zhang H, Huang Y, Yang G, Du M, et al. Dietary grape seed extract ameliorates symptoms of inflammatory bowel disease in IL10-deficient mice. *Mol Nutr Food Res* 2013;57:2253–7.
- [17] Yousef MI, Saad AA, El-Shennaway LK. Protective effect of grape seed proanthocyanidin extract against oxidative stress induced by cis-platin in rats. *Food Chem Toxicol* 2009;47:1176–83.
- [18] Osman HA. Morphological evaluation on the protective effect of curcumin on nicotine induced histological changes of the adrenal cortex in mice. *Egypt J Histol* 2010;33:552–9.
- [19] Bancroft JD, Layton C. Bancroft's theory and practice of histological techniques. 7th ed. Oxford: Elsevier Churchill Livingstone; 2013. p. 173–86.
- [20] Vosse BAH, Seelentag W, Bachmann A, Bosman FT, Yan P. Background staining of visualization systems in immunohistochemistry. *Appl Immunohistochem Mol Morphol* 2007;15:103–7.
- [21] Kamel ZM, Attia MM, Deiaa EM, Gamal AA. Enhancement of neural stem cells after induction of depression in male albino rats (a histological & immunohistochemical study). *Int J Stem Cells* 2014;7:70–8.
- [22] Bancroft JD, Gamble M. Theory and practice of histological technique. 6th ed. London, New York: Elsevier Churchill Livingstone; 2008. p. 121–7.
- [23] Sabha MJ, Emirandetti A, Cullheim S, Oliveira ALR. MHC1 expression and synaptic plasticity in different mice strains after axotomy. *Synapse* 2008;62:137–48.
- [24] Ramesh G, Reeves WB. p38 MAP kinase inhibition ameliorates cisplatin nephrotoxicity in mice. *Am J Physiol Renal Physiol* 2005;289:F166–74.
- [25] Wilcox RR. Basic statistics: understanding conventional methods and modern-insights. 1st ed. Oxford, New York: Oxford University Press; 2009. p. 210–30.
- [26] U.S. Department of Health and Human Services. The health consequences of smoking—50 years of progress: a report of the surgeon general. Atlanta, GA: U.S. Department of Health and Human Services, Centers for Disease Control and Prevention, National Center for Chronic Disease Prevention and Health Promotion, Office on Smoking and Health; 2014.
- [27] Senthilkumar R, Viswanathan P, Nalini N. Effect of glycine on oxidative stress in rats with alcohol induced liver injury. *Pharmazie* 2004;59:55–60.
- [28] Elshennawy WW, Aboelwafa RH. Structural and ultrastructural alterations in mammalian adrenal cortex under influence of steroidogenesis inhibitors drug. *J Am Sci* 2011;7(8):567–76.
- [29] Thomas M, Keramidas M, Monchaux E, Feige JJ. Dual hormonal regulation of endocrine tissue mass and vasculature by adrenocorticotropin in the adrenal cortex. *Endocrinology* 2004;145:4320–9.
- [30] Wang H, Huang M, Peng RX, Le J. Influences of 3-methylcholanthrene, phenobarbital and dexamethasone on xenobiotic metabolizing-related cytochrome P450 enzymes and steroidogenesis in human fetal adrenal cortical cells. *Acta Pharmacol Sin* 2006;27:1093–6.
- [31] Miller WL, Auchus RJ. The molecular biology, biochemistry, and physiology of human steroidogenesis and its disorders. *Endocr Rev* 2011;32:81–151.
- [32] Wang T, Chen M, Liu L, Cheng H, Yan Y, Feng Y, et al. Nicotine induced CpG methylation of Pax6 binding motif in StAR promoter reduces the gene expression and cortisol production. Paper 90, Uniformed Services University of the Health Sciences 2011.
- [33] Green DR, Kroemer G. The pathophysiology of mitochondrial cell death. *Science* 2004;30:626–9.
- [34] Luiz F, Camila R, Carla C, Ricardo S, Maria C, José M, et al. Melatonin action in apoptosis and vascular endothelial growth factor in adrenal cortex of pinealectomized female rats. *Rev Bras Ginecol Obstet* 2010;32(8):374–80.
- [35] Kim KH, Joo KJ, Park HJ, Kwon CH, Jang MH, Kim CJ. Nicotine induces apoptosis in TM3 mouse Leydig cells. *Fertil Steril* 2005;83:1093–9.
- [36] Machaalani R, Waters KA, Tinworth KD. Effects of postnatal nicotine exposure on apoptotic markers in the developing piglet brain. *Neuroscience* 2005;132:325–33.
- [37] Kang SW, Park HJ, Ban JV, Chung JH, Chun GS, Cho JO. Effects of nicotine on apoptosis in human gingival fibroblasts. *Arch Oral Biol* 2011;56:1091–7.
- [38] Iranlooye BO, Bolarinwa AF. Effect of nicotine administration on weight and histology of some visceral organs in female albino rats. *Niger J Physiol Sci* 2009;24:7–12.
- [39] Razali N, Junit SM, Ariffin A, Ramli NSF, Aziz AA. Polyphenols from the extract and fraction of *T. indica* seeds protected HepG2 cells against oxidative stress. *BMC Complement Altern Med* 2015;15:1–16.
- [40] Parlakpinar H, Tasdemir S, Polat A, Bay-Karabulut A, Vardi N, Ucar M, et al. Protective role of caffeic acid phenethyl ester (CAPE) on gentamicin-induced acute renal toxicity in rats. *Toxicology* 2005;2:169–77.
- [41] Balakrishnan A, Menon V. Protective effect of hesperidin on nicotine induced toxicity in rats. *Indian J Exp Biol* 2007;45:194–202.
- [42] Barr J, Sharma CS, Sarkar S, Wise K, Dong L, Periyakaruppan A, et al. Nicotine induces oxidative stress and activates nuclear transcription factor kappa B in rat mesencephalic cells. *Mol Cell Biochem* 2007;297:93–9.
- [43] Wang H, Ma L, Li Y, Cho CH. Exposure to cigarette smoke increases apoptosis in the gastric mucosa through a reactive active species mediated and P-53 independent pathway. *Free Radic Biol Med* 2000;28:1295.
- [44] Ahmed HH, Abdel-fatah HM, Hamza AH, Mahmoud RH. Grape seed extract restrains hepatocellular carcinoma: pre-clinical study. *Int J Pharm Biosci* 2015;6:514–25.
- [45] Zhang J, Pan X, Wang Y, Liu X, Yin X, Yu Z. Grape seed extract attenuates arsenic-induced nephrotoxicity in rats. *Exp Ther Med* 2014;7:260–6.
- [46] Nada SA, Eldenshary ES, Abdel Salam OME, Azmy SA, Mahdy T, Galal AF, et al. Grape seed extract attenuate tramadol-alcohol hepatotoxicity and increased antioxidant status in Sprague Dawley rats. *Curr Sci Int* 2014;3:260–70.
- [47] Nesseim WH, Haroun HS, Mostafa E, Youakim MF, Mostafa M. Effect of nicotine on spermatogenesis in adult albino rats. *Andrologia* 2011;43:398–404.
- [48] El-Meligy MS, Abdel Hady RH, Abdel Samaei A, Saad Eldien HM. Effect of nicotine administration and its withdrawal on the reproductive organs, fertility, and pregnancy outcome in female rats. *Mansoura J Forensic Med Clin Toxicol* 2007;1:95–130.